Dalton Transactions

Accepted Manuscript

ROYAL SOCIETY OF CHEMISTRY

www.rsc.org/dalton

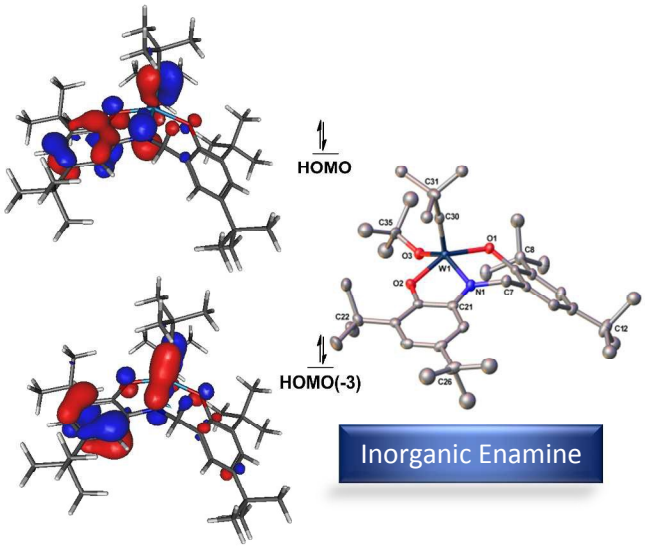

Inorganic Enamine

Journal Name

ARTICLE

A New ONO^{3-} Trianionic Pincer Ligand with Intermediate Flexibility and its Tungsten Alkylidene and Alkylidyne Complexes

Received 00th January 20xx,
Accepted 00th January 20xx

DOI: 10.1039/x0xx00000x

www.rsc.org/

Sudarsan VenkatRamani,[a] Ion Ghiviriga,[a] Khalil A. Abboud,[a] and Adam S. Veige[a]

This report details the synthesis and characterization of the semi-flexible [ON^{CH2}O]H$_3$ (**1**) ligand and its W(VI)-alkylidene and alkylidyne complexes. The alkylidyne complex [ON*H*^{CH2}O]W≡C^{t}Bu(O^{t}Bu) (**2**) forms as a result of alcoholysis of **1** with (^{t}BuO)$_3$W≡C^{t}Bu. Complex **2** evolves to [ON^{CH2}O]W=C*H*^{t}Bu(O^{t}Bu) (**3**) through proton migration from the N atom of the pincer ligand to the to W≡C$_\alpha$ bond. Deprotonation of **2** or **3** with Ph$_3$PCH$_2$ affords the anionic alkylidyne {CH$_3$PPh$_3$}{[ON^{CH2}O]W≡C^{t}Bu(O^{t}Bu)} (**4**). Complex **4** exhibits pincer-ligand–centered reactivity with electrophiles (H$^+$, Me$^+$, and TMS$^+$), in spite of its enhanced inorganic enamine interaction. Addition of 2 equiv of HCl to **4** yields the W(VI)-neopentyl complex [ON^{CH2}O]W(CH$_2$^{t}Bu)(O^{t}Bu)(Cl) (**5**). MeOTf or TMSOTf addition to **4** generates the dianionic pincer ligated alkylidynes [ON*R*^{CH2}O]W≡C^{t}Bu(O^{t}Bu) (R = Me (**6-Me**); TMS (**6-TMS**)). Complexes **2** – **5** were characterized by multinuclear NMR spectroscopy, and combustion analysis. Complexes **4** and **5** were also characterized by single crystal X-ray diffraction. This work bridges the gap in the series involving W(VI)-alkylidynes ligated to the rigid [CF$_3$-ONO]$^{3-}$, and the flexible [O^{CH2}N^{CH2}O]$^{3-}$ ligands. DFT computations permit comparison of the inorganic enamine effect within alkylidynes supported by all three trianionic-pincer type ONO ligands.

Introduction

Monodentate amido ligands (M–NR$_2$, R = H, alkyl, aryl) are strong π-donors by virtue of the lone pair of electrons residing on the N atom. When appended to a metal alkylidyne, and given the opportunity to freely rotate around the M–N bond, the preferential orientation is for the lone pair of electrons to donate into an empty metal d-orbital to maximize orbital overlap (**Figure 1**; Case A).[1-6] An interesting consequence arises by forcibly constraining the amido lone pair to be collinear with metal-carbon multiple bonds. In the most straightforward scenario, the amido lone pair creates a bonding and an 'anti-bonding combination with the M–C π-bond (**Figure 1**; Cases B - D).[7-9]

Constraining the amido lone pair to be collinear to the M–C π-bonds has two important electronic consequences: 1) the HOMO orbital is destabilized, and 2) electron density is delocalized from the amido lone pair onto the α-carbon of the metal-carbon multiple bond. The destabilization of the HOMO coupled to increased electron density on the carbon should, in principle, lead to alkylidenes and alkylidynes with enhanced nucleophilicity. This orbital overlap combination is termed an inorganic enamine[7-9] due to its isolobal relationship with the well-studied enhanced nucleophilicity of organic enamines.[10]

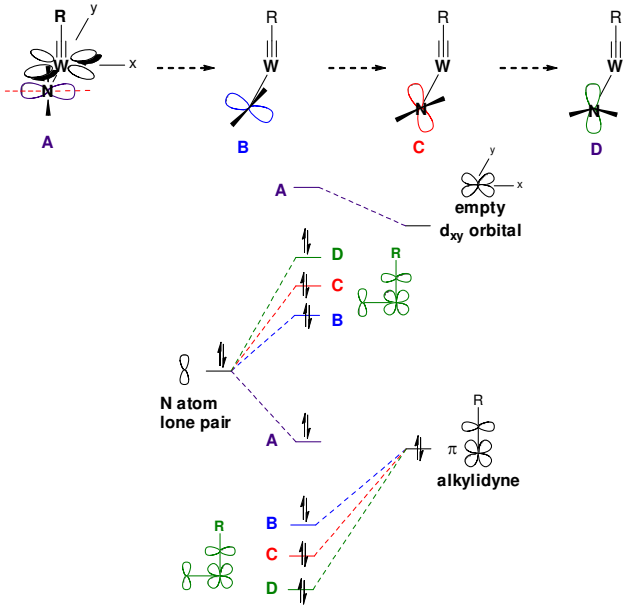

Figure 1. Top: orientation of amido lone pair with respect to the alkylidyne π-orbitals: unrestricted (Case A; e.g., monodentate amido ligands) to constrained (Cases B-D; within a trianionic pincer-type [ONO]$^{3-}$ ligand framework). Bottom: truncated qualitative orbital diagram for cases A-D (bonding and anti-bonding combinations depicted). Separation between bonding and anti-bonding orbitals varies as a function of the amido lone pair orientation with alkylidyne π-orbitals.

Trianionic ONO pincer-type ligands provide the necessary constraint to orient the N atom lone-pair to be collinear with

Department of Chemistry, Center for Catalysis, University of Florida, Gainesville, Florida, 32611(USA). E-mail: veige@chem.ufl.edu; Tel.: +1 352-392-9844; Fax: +1 352-392-3255

Electronic Supplementary Information (ESI) available: NMR spectra, X-ray crystallographic data, and experimental procedure for 1-6. CCDC reference numbers 1415361 (**5**), 1415362 (**4**). For ESI and crystallographic data in CIF or other electronic format see DOI: 10.1039/x0xx00000x

metal-carbon multiple bonds. Indeed, DFT computations of the anionic complex $\{CH_3PPh_3\}\{[CF_3\text{-}ONO]W{\equiv}CEt(O^tBu)\}$[7] (

Figure **2A**) reveal orbital overlap between the N atom lone pair and one of the metal-carbon π-bonds. In addition, the neutral complex $[CF_3\text{-}ONO]W{\equiv}C^tBu(THF)_2$ exhibits Wittig-like chemistry with carbonyl-containing substrates that are up to four orders of magnitude faster than $(DIPP)_3W{\equiv}C^tBu$ (DIPP = 2,6-diisopropylphenoxide).[11] Prepared recently, the more flexible ONO ligand within complex $\{CH_3PPh_3\}\{[[O^{CH2}N^{CH2}O]W{\equiv}C^tBu(O^tBu)\}$[9] (

Figure **2B**) also contains an inorganic enamine bonding combination, perhaps even to a greater extent than $\{CH_3PPh_3\}\{[CF_3\text{-}ONO]W{\equiv}CEt(O^tBu)\}$; however, access to the neutral species was hampered since electrophilic additions occur at the exposed N atom rather than the sterically protected alkylidyne. In this work, we present the synthesis and characterization of the new *intermediate* flexible trianionic ONO pincer ligand $[ON^{CH2}O]H_3$ (**1**) and its tungsten-alkylidene $[ON^{CH2}O]W{=}CH^tBu(O^tBu)$ (**3**) and -alkylidyne $\{CH_3PPh_3\}\{[ON^{CH2}O]W{\equiv}C^tBu(O^tBu)\}$ (**4**) complexes. DFT computations permit a comparison between anionic W(VI) alkylidynes comprising the rigid $\{[CF_3\text{-}ONO]^{3-}$, intermediate $[ON^{CH2}O]^{3-}$, and flexible $[O^{CH2}N^{CH2}O]^{3-}$ trianionic ONO pincer-type ligands and their influence on the magnitude of the inorganic enamine.

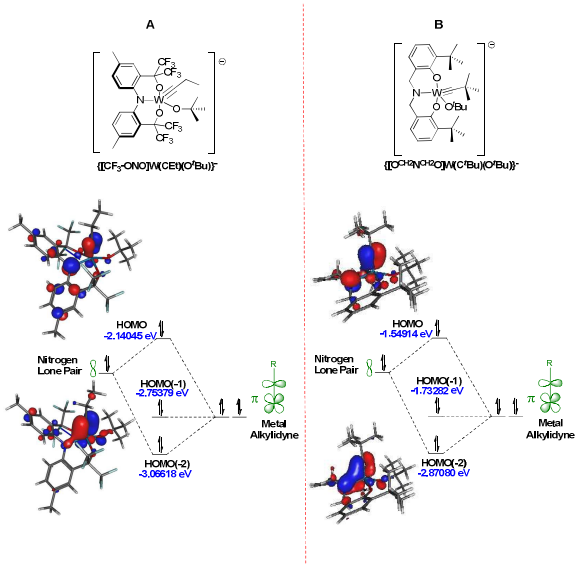

Figure 2. Comparison of the inorganic enamine bonding combinations in the rigid $\{[CF_3\text{-}ONO]W{\equiv}CEt(O^tBu)\}^-$ (**A**),[7] and flexible $\{[O^{CH2}N^{CH2}O]W{\equiv}C^tBu(O^tBu)\}^-$ (**B**) anions. Orbital images generated at isovalue 0.051687.

Results

Multi-gram quantities of proligand **1** are accessible from readily available starting materials through a straightforward condensation reaction to generate first an imine intermediate, followed by reduction. In a single step, without need for further purification, treating 2-amino-4,6-di-tert-butylphenol[12-15] with 3,5-di-tert-butyl-2-hydroxybenzaldehyde[16-18] provides the imine, 2,4-di-tert-butyl-6-((3,5-di-tert-butyl-2-hydroxybenzylidene)amino)phenol,[19-23] (**Scheme 1**). Treating the imine, isolated as a pale yellow microcrystalline solid, with excess sodium borohydride[21, 24] provides the corresponding secondary amine and the proligand **1** as the hydrochloride salt **1·HCl** as a pale pink solid. Treating **1·HCl** in methanol with a methanolic solution of anhydrous sodium methoxide generates the proligand **1** in 52% yield.

Scheme 1. Synthesis of $[ON^{CH2}O]H_3$ (**1**)[a]

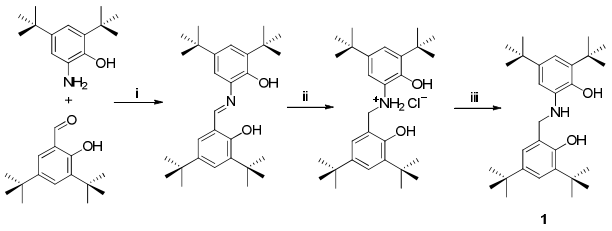

[a]Legend: (i) EtOH (200 proof), 5 h reflux, 2 drops HAc; (ii) 4 equiv $NaBH_4$, 2 h reflux; dil. HCl; (iii) 1 equiv NaOMe(s), MeOH; pentane recrystallization.

^{1}H-NMR spectroscopy confirms the identity of **1** as a C_1-symmetric compound. In benzene-d_6, the methylene protons, resonating as a singlet at 3.89 ppm, confirm the presence of the secondary amine. The four ^{t}Bu groups resonate as distinct singlets at 1.29, 1.39, 1.40, and 1.65 ppm. Aromatic protons, also demonstrating the low-symmetry of **1** resonate as four distinct doublets centered at 6.83, 6.94, 7.10 and 7.51 ppm. Further evidence for the identity of **1** comes from 2D NMR experiments. ^{1}H-^{15}N *g*HMBC analysis indicates, via a cross-peak with an aromatic proton at 6.83 ppm, that the N atom in **1** resonates at 50.0 ppm, which is consistent with N atom in the symmetric $[CF_3\text{-}ONO]H_3$[7] ligand that resonates at 66.2 ppm.

Treating a benzene solution of **1** with $(^tBuO)_3W{\equiv}C^tBu$[2, 25] produces the dianionic pincer-type alkylidyne $[ONH^{CH2}O]W{\equiv}C^tBu(O^tBu)$ (**2**) initially; however, left in solution, **2** slowly converts to the trianionic pincer-type alkylidene complex $[ON^{CH2}O]W{=}CH^tBu(O^tBu)$ (**3**). For example, stirring a benzene solution composed of the proligand **1** and the tungsten precursor $(^tBuO)_3W{\equiv}C^tBu$ overnight, provides predominantly **3**, with little or none of **2** (**Scheme 2**).

Scheme 2. Syntheses of [ON*H*^{CH2}O]W≡C^{t}Bu(O^{t}Bu), (**2**) and [ON^{CH2}O]W=CH^{t}Bu(O^{t}Bu), (**3**)

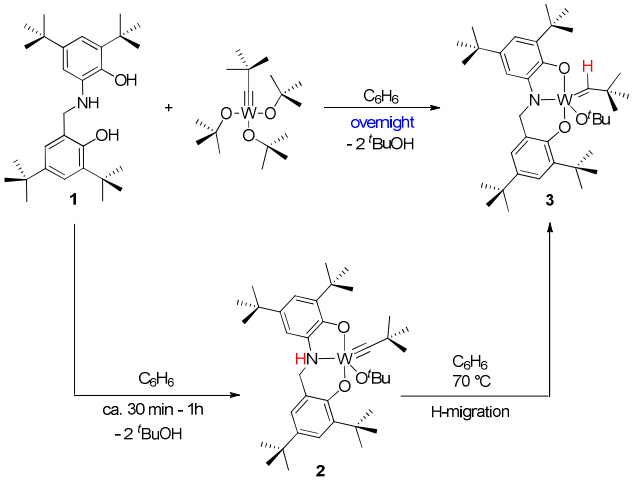

Combining benzene solutions of **1** with (^{t}BuO)$_3$W≡C^{t}Bu, but stopping the reaction after 30 min, allows for the clean isolation of the dianionic pincer-type alkylidyne complex [ON***H***^{CH2}O]W≡C^{t}Bu(O^{t}Bu) (**2**). The ^{1}H NMR spectrum of **2** (at –30 °C in toluene-d_8 or in C_6D_6 at 25 °C) exhibits resonances consistent with a C_1-symmetric complex. Most notably, the amine proton resonates at 2.79 ppm (toluene-d_8 at –30 °C) as a broad doublet of doublets due to coupling to the adjacent methylene protons. Consequently, the methylene protons, being diastereotopic, appear as two doublets of doublets centered at 4.78 and 4.97 ppm. The resonance at 4.97 ppm is *anti* to the amine protons and exhibits a large vicinal coupling constant ($^3J_{HH}$) of 12.9 Hz with the amine proton. The resonance at 4.78 ppm corresponds to the *syn* proton since it exhibits much smaller vicinal coupling of 1.8 Hz.[26-27] The ^{t}Bu group bound to the W≡C$_\alpha$ resonates as a singlet at 0.82 ppm. Further evidence for the stereochemical assignment of the amine and methylene protons comes from a 1D-NOE experiment. Selective inversion of the resonance at 0.82 ppm (W≡C^{t}Bu) displays an NOE with the methylene proton at 4.97 ppm, confirming its *syn* orientation with respect to the ^{t}Bu moiety. The NH proton, by virtue of its large coupling constant ($^3J_{HH}$ = 12.9 Hz), with the methylene resonance at 4.97 ppm, must therefore be *anti*-disposed.[26-27] In the ^{13}C{^{1}H} NMR spectrum of **2**, a resonance at 288.5 ppm (toluene-d_8 at – 30 °C) offers conclusive proof for the persistence of the alkylidyne moiety in solution.[1-3, 7-9, 28-34] The N atom, being an L-type donor,[35] resonates at 48.1 ppm in the ^{1}H-^{15}N *g*HMBC NMR spectrum.

The dianionic alkylidyne [ON***H***^{CH2}O]W≡C^{t}Bu(O^{t}Bu) (**2**), when heated to 70 °C for 5 h in C_6D_6, evolves into the thermodynamic product, the trianionic pincer-type alkylidene [ON^{CH2}O]W=C***H***^{t}Bu(O^{t}Bu) (**3**). ^{1}H NMR spectroscopy provides a method for monitoring the quantitative conversion of **2** into **3** (see Figure S10). Pertinent resonances within **3** that serve as unique spectroscopic handles include the ^{t}Bu group bound to the W=C$_\alpha$ resonating at 0.68 ppm, the methylene protons resonating as two doublets centered at 5.08 and 5.46 ppm, and most importantly, the alkylidene proton W=C***H***^{t}Bu, resonating as a singlet at 8.90 ppm with satellite coupling to ^{183}W isotope ($^2J_{WH}$ = 15.5 Hz). Confirming the change in unsaturation of the C$_\alpha$, the W=***C***$_\alpha$ resonates at 255.6 ppm for **3**, in contrast to the W≡***C***$_\alpha$ in **2**, which resonates downfield at 288.5 ppm. The N atom in **3**, now an X-type donor,[35] resonates at 260.6 ppm in the ^{1}H-^{15}N *g*HMBC spectrum, a dramatic shift downfield compared to 48.1 for **2**.

Alkylidyne [ON***H***^{CH2}O]W≡C^{t}Bu(O^{t}Bu) (**2**), similar to the previously reported dianionic pincer alkylidynes [O^{CH2}NH^{CH2}O]W≡CR(O^{t}Bu) (where R = Et, ^{t}Bu),[9] retains the proton on the N atom. The N atom in the flexible ligand [O^{CH2}N^{CH2}O]H$_3$[9] is an aliphatic secondary amine, and also the most basic site. Much like the [CF$_3$-ONO]H$_3$ and [pyr-ONO]H$_3$ ligands,[7-8, 32] the proton on the N atom in **2** eventually migrates to the W≡C unit, generating the corresponding alkylidene **3**, the thermodynamic product.

Adding phosphorane (Ph$_3$P=CH$_2$)[36] to either **2** or **3**, or as a mixture of the two complexes, readily generates the trianionic alkylidyne complex **4** in excellent yields (96%) (**Scheme 3**). Complex **4** precipitates from pentane allowing for easy isolation with relatively little additional work-up.

Scheme 3. Synthesis of {CH$_3$PPh$_3$}{[ON^{CH2}O]W≡C^{t}Bu(O^{t}Bu)} **(4)**

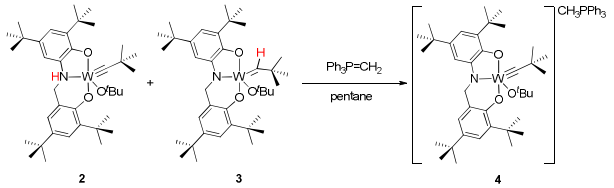

The ^{1}H NMR spectrum (C_6D_6) of **4** confirms the formation of the trianionic alkylidyne complex. The ^{t}Bu group on the W≡C$_\alpha$ unit serves as the diagnostic handle; within **4**, the ^{t}Bu protons resonate at 1.15 ppm in contrast to **2** (0.82 ppm) and **3** (0.68 ppm). The methylene proton resonances shift slightly upfield as compared to those in **3**, and appear as two distinct doublets centered at 5.05 and 5.37 ppm. The resonances from the phosphonium cation are broad with the methyl protons appearing at 2.27 ppm (2.55 ppm in THF-d_8). Broad phosphonium cation signals were also observed for the anionic alkylidyne {CH$_3$PPh$_3$}{[O^{CH2}N^{CH2}O]W≡C^{t}Bu(O^{t}Bu)}.[9] Both ^{13}C{^{1}H} and ^{31}P{^{1}H} NMR spectroscopies further corroborate the identity of **4**. The W≡C$_\alpha$ unit resonates at 290.6 ppm, and is consistent with previously characterized W(VI)-alkylidynes.[1-3, 7-9, 28-34] A singlet resonance for the phosphonium cation at 21.7 ppm in the ^{31}P{^{1}H} NMR spectrum agrees with similar anionic alkylidynes with phosphonium counter cations.[7,24,36-38,43] The most conclusive evidence for the identity of **4** comes from X-ray crystallographic interrogation of single crystals that grow from pentane diffusion into a saturated THF solution of **4**.

The molecular structure of **4**, depicted in **Figure 3**, comprises the W(VI) ion residing at the center of a distorted-square-pyramid (τ = 0.09),[37] with the [ON^{CH2}O]$^{3-}$ ligand, and the –O^{t}Bu ligand forming the square base. The alkylidyne ligand (W≡**C^{t}Bu**) occupies the apical position. The methyl groups on

carbon atoms C12, C26, C31, and C35 are disordered, and were dependently refined in two parts. The methylene protons on C7 were obtained from the difference Fourier map and refined freely. The sum of the angles around N1 of 359.22(24)° suggests a planar sp^2-hybridized N atom. Indeed, the N1–W1 bond length of 2.085(2) indicates an anionic nitrogen (X-type donor);[35] this bond length agrees well with similar anionic N atoms in the W(VI) alkylidyne complexes $\{CH_3PPh_3\}\{[O^{CH2}N^{CH2}O]W{\equiv}C^tBu(O^tBu)\}$ with N1–W1 = 2.026(3) Å,[9] $\{CH_3PPh_3\}\}\{[pyr\text{-}ONO]W{\equiv}C^tBu(O^tBu)\}$ with N1–W1 = 2.161(3) Å,[32] and the neutral W-alkylidyne complex $[CF_3\text{-}ONO]W{\equiv}C^tBu(OEt_2)$ with a N1–W1 bond length of 2.008(2) Å.[8] The vector perpendicular to the C21–N1–C7 plane represents the idealized position of the nitrogen lone pair; in **4**, the N atom lone pair exhibits a 7° deviation from coplanarity with the W≡C bond. An angle of 7° is overwhelmingly the smallest deviation compared to similar anionic alkylidynes supported by the rigid $[CF_3\text{-}ONO]^{3-}$ (θ = 43°), and the flexible $[O^{CH2}N^{CH2}O]^{3-}$ (θ = 44°) ligands.[7-9]

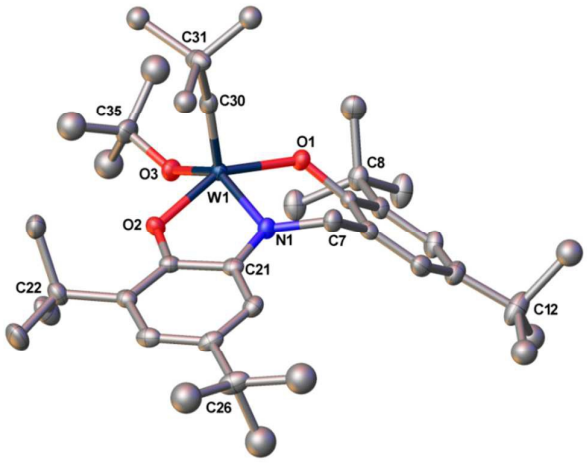

Figure 3. Molecular structure of **4** with hydrogen atoms, disordered methyl groups on C12 / C26/ C31/ C35, and phosphonium cation removed for clarity. Selected bond distances (Å): W1–C30 1.757(3), C30–C31 1.513(4), W1–O1 1.9771(18), W1–O2 1.9918(18), W1–O3 1.9161(18), W1–N1 2.085(2), N1–C7 1.462(3), N1–C21 1.391(3). Selected bond angles (deg): ∠W1–C30–C31 159.7(2), ∠W1–O3–C35 139.27(16), ∠N1–W1–O3 144.38(8), ∠O1–W1–O2 150.09(8), ∠C21–N1–C7 120.2(2), ∠C21–N1–W1 117.82(17), ∠C7–N1–W1 121.21(18).

Another striking difference in the molecular structure of **4** is the ∠W1–C30–C31 angle within the alkylidyne ligand, measuring 159.7°(2). Similar W(VI)-alkylidynes featuring $W{\equiv}C^tBu$ groups, all exhibit a nearly linear ∠W≡C–C angle, ranging between 170 - 175°.[1-3, 8, 30, 32, 38-40] The closest evidence for a high valent W-alkylidyne that shows significant deviation in its ∠W≡C–C angle is the complex $CpW{\equiv}CAd(CH_2{}^tBu)_2$ reported by Schrock;[41] this complex, bearing an adamantyl unit on the $W{\equiv}C_\alpha$ features an acute ∠W≡C–C angle of 166.2(6)°. The complexes $TpW{\equiv}C^tBu(NHPh)_2$ (Boncella et al.; ∠W≡C–C angle = 166.5(4)°)[42] and $Tp^*W{\equiv}CPh(Br)_2$ (McCleverty et al.; ∠W≡C–C angle = 168.0(8)°)[43] also exhibit ∠W≡C–C angles that deviate significantly from linearity. The ∠W≡C–C angle in the complex $(^{Me2}Im)((CF_3)_2(CH_3)CO)_2W{\equiv}CPh$ reported by Tamm et al. measures 169.9(5)°.[29] The small angle in **4** is due to packing forces. Tamm's complex $(^{DIPP}Im)((CF_3)_2(CH_3)CO)_2W{\equiv}C^tBu$ exhibits an angle of 168.8(2);[2] however, this is only one of the two independent molecules present in the asymmetric unit. The other molecule in the asymmetric unit exhibits a typical ∠W≡C–C angle of 175.2(3)°. The difference in the angles between two identical molecules within the asymmetric unit provides compelling evidence that the acute angle is simply a consequence of crystal packing forces. Finally, in **4**, the W1≡C30 bond length is 1.757(3) Å, a value consistent with other W≡C bond lengths that range between 1.745 – 1.838 Å.[1-5, 28-29, 41, 44-52]

DFT computation of $\{CH_3PPh_3\}\{[ON^{CH2}O]W{\equiv}C^tBu(O^tBu)\}$(4)

Ground state DFT calculations (geometry optimization and single point analysis) were performed on **4**, employing the hybrid functional B3LYP[53-54] / LANL2DZ[55] basis sets from the Gaussian 09[56] program suite; the atomic coordinates of **4**, generated from the X-ray crystallography experiment, served as the initial input. Molecular orbitals were generated using Gabedit[57] at the specified isovalues. As is evident from **Figure 4** and **Table 1**, the structural parameters of the computed structure **4a** show good agreement with the experimentally observed values. For example, the sum of the angles around the N atom in **4a** sum to 359.25°, agreeing well with the experimental value of 359.22(24)°, and the N1-W1 bond length computes to 2.104 Å, showing only a ~0.02 Å deviation from the experimental value of 2.085(2) Å. The calculation also correctly estimates the W1–C30 bond length as 1.780 Å, with only a ~0.02 Å deviation from the experimental value. In the absence of crystal packing forces, the ∠W1–C30–C31 angle returns to the normal value of 172.20° in **4a**.

As previously mentioned, the nitrogen atom lone pair in the solid state structure of **4** is 7° from being collinear with the alkylidyne π-orbitals. The geometry-optimized structure **4a**, however, shows a slightly larger deviation. The vector perpendicular to the C7–N1–C21 plane representing the idealized position of the nitrogen lone pair is roughly 14° away from being collinear to the alkylidyne π-orbitals in **4a**. An important consequence of the nearly collinear arrangement is the overlap of the amido lone pair with the alkylidyne π-orbitals; the bonding interaction generates an *inorganic enamine* (see HOMO(-3), and the HOMO in **Figure 5**).[10]

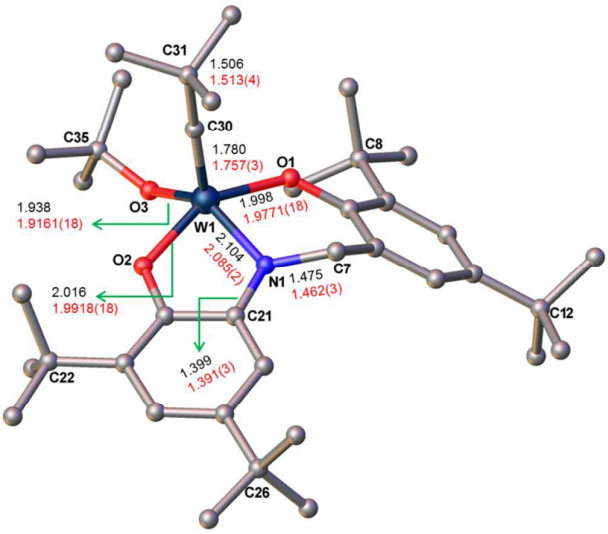

Figure 4. Geometry-optimized structure of **4a** employing the hybrid functional B3LYP/ LANL2DZ basis sets

Table 1. Selected Bond Lengths (Å) and Angles (deg) for the Single-Crystal X-ray Structure of **4** and DFT Geometry-Optimized Structure of **4a**

Bond length	**4**	**4a**$_{(B3LYP/LANL2DZ)}$
W1–C30	1.757(3)	1.780
C30–C31	1.513(4)	1.506
W1–O1	1.9771(18)	1.998
W1–O2	1.9918(18)	2.016
W1–O3	1.9161(18)	1.938
W1–N1	2.085(2)	2.104
N1–C7	1.462(3)	1.475
N1–C21	1.391(3)	1.399
Bond angle	**4**	**4a**$_{(B3LYP/LANL2DZ)}$
∠W1–C30–C31	159.7(2)	172.20
∠W1–O3–C35	139.27(16)	143.44
∠N1–W1–O3	144.38(8)	144.35
∠O1–W1–O2	150.09(8)	150.18
∠C21–N1–C7	120.2(2)	120.16
∠C21–N1–W1	117.82(17)	117.99
∠C7–N1–W1	121.21(18)	121.10

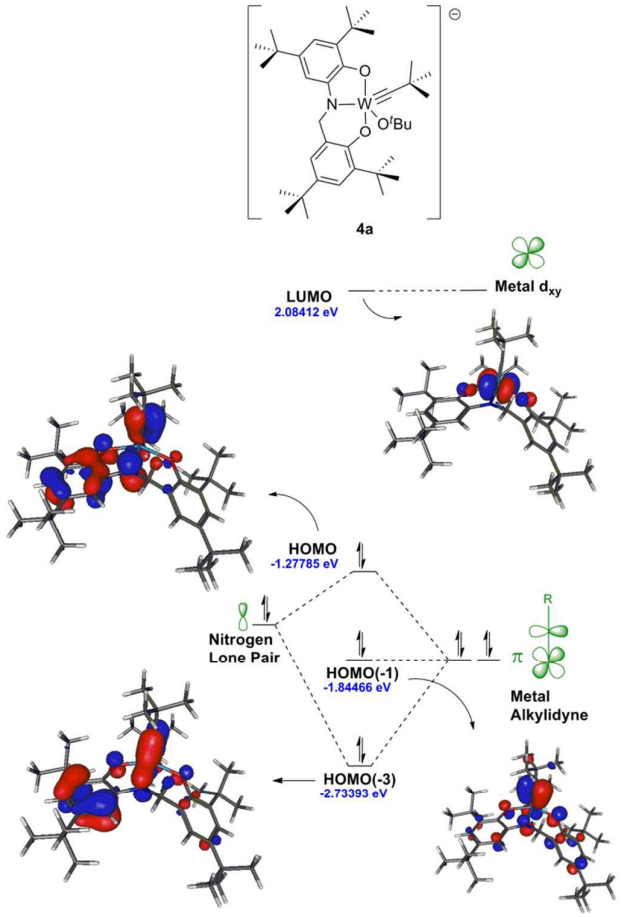

Figure 5. Truncated molecular orbital diagram of **4a** (B3LYP / LANL2DZ level theory). The HOMO and HOMO(-3) of **4a** exhibits the inorganic enamine combination. (isovalue 0.041687).

In situ addition of electrophiles to 4 and solution phase characterization

The anionic alkylidyne, {[ON^{CH2}O]W≡C^{t}Bu(O^{t}Bu)}$^{-}$ (**4**) bears structural similarities to the previously studied complex {[O^{CH2}N^{CH2}O]W≡C^{t}Bu(O^{t}Bu)}$^{-}$.[9] The presence of the methylene spacers within {[O^{CH2}N^{CH2}O]W≡C^{t}Bu(O^{t}Bu)}$^{-}$ leave the N atom exposed, predisposing it to preferential N-centered reactivity.[9] Complex **4** was treated with electrophiles of varying sizes to assess its reactivity patterns.

Addition of H+. Addition of one equivalent of HCl (as a diethyl ether solution) to a C_6D_6 solution of **4** readily generates the neopentylidene complex [ON^{CH2}O]W=CH^{t}Bu(O^{t}Bu) (**3**). The appearance of a resonance at 8.90 ppm in the ^{1}H NMR spectrum is characteristic of the alkylidene product **3**, rather than the kinetic product **2**, described above. Addition of a second equivalent of HCl to **3** further protonates the W=CH(^{t}Bu) unit to generate the W-neopentyl complex [ON^{CH2}O]WCH$_2$^{t}Bu(O^{t}Bu)(Cl) (**5**) (**Scheme 4**). The disappearance of the resonance for the alkylidene proton at 8.90 ppm in the ^{1}H NMR spectrum coincides with the emergence of a second pair of doublets. The doublets centered at 2.20 and 2.41 ppm are attributable to the CH$_2$ protons on the W–CH$_2$^{t}Bu ligand

and integrate to one proton each relative to nine for the ^{t}Bu protons that resonate at 0.96 ppm. Double protonation of the alkylidyne π-bonds in **4** is different from the reactivity of the prototypical Schrock alkylidyne $(^t\text{BuO})_3\text{W}{\equiv}\text{C}^t\text{Bu}$, which reacts with two equivalents of HX (X = Cl, Br) to form $(\text{O}^t\text{Bu})_2\text{W}{=}\text{CH}^t\text{Bu(X)}_2$.[58] An alternative, and perhaps a more straightforward approach to the synthesis of **5** involves reacting **1·HCl** directly with $(^t\text{BuO})_3\text{W}{\equiv}\text{C}^t\text{Bu}$ in benzene (**Scheme 4**).

Scheme 4. Synthesis of **5** either through protonation of **4** or from **1·HCl**

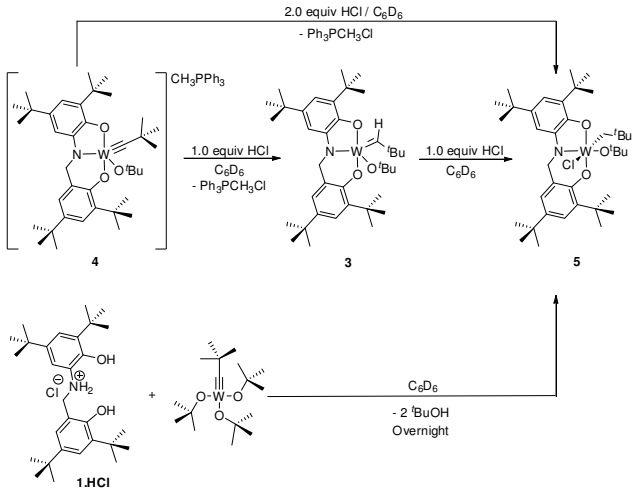

Crystals suitable for an X-ray diffraction experiment grow from a saturated diethyl ether solution of **5**. Depicted in **Figure 6** is the solid state molecular structure of **5**. In **5**, the W(VI) ion resides in a distorted octahedral environment with the $[\text{ON}^{\text{CH2}}\text{O}]^{3-}$ and $-\text{O}^t\text{Bu}$ ligands comprising one plane and the neopentyl and chloride ligands occupy *trans* positions. The methyl groups on carbon atoms C12, and C26 are disordered and were each refined in two parts. The two methylene protons on C30 were located in the difference Fourier map and refined freely. The sum of the angles around the nitrogen atom of 359.64(27)°, and a short N1–W1 bond length of 2.015(2) Å, suggest a planar sp^2-hybridized anionic nitrogen (i.e. X-type donor).[35] Further support for an anionic N atom within the pincer is its downfield resonance at 299.8 ppm observed in the ^{1}H-^{15}N *g*HMBC NMR spectrum.

The W-imido complex $[\{o\text{-C}_6\text{H}_4(\text{NSiMe}_3)_2\}\text{W}{\equiv}\text{NPh(Cl)(CH}_2{}^t\text{Bu)}]$[22] is the closest reported structure to **5**. The W1–Cl1 bond length of 2.5221(7) Å in **5** is in agreement with the W1–Cl1 bond length of 2.422(2) Å in the W-imido complex. Similarly, the W1–C30 bond distance of 2.172(3) Å and the ∠W1–C30–C31 angle of 126.3(2)° agree with the corresponding metric parameters of 2.182(4) Å and 126.1(4)° within the W-imido complex, respectively. The W1–C30 bond distance of 2.172(3) Å for the W–neopentyl ligand in **5** is shorter than the corresponding value of 2.258(8) Å found in the W-neopentyl-neopentylidene-neopentylidyne complex, $(\text{DMPE})\text{W(CH}_2\text{C}^t\text{Bu)(=CH}^t\text{Bu)(}{\equiv}\text{C}^t\text{Bu)}$.[39, 59] Complex **5** is stable to excess HCl (as a diethyl ether solution) up to a week; even heating to 50 °C does not produce the corresponding dichloride $[\text{ON}^{\text{CH2}}\text{O}]\text{W(Np)Cl}_2$.

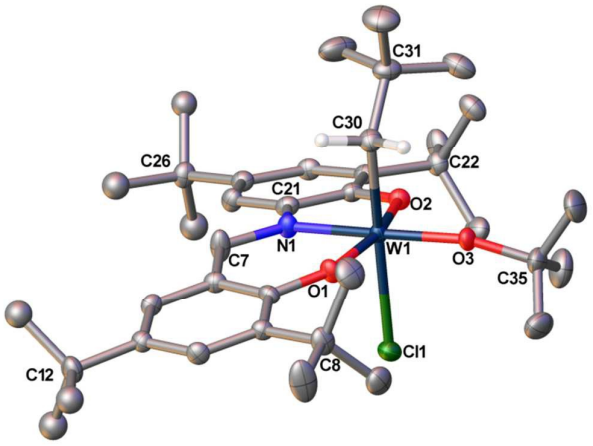

Figure 6. Solid state molecular structure of **5**, with hydrogen atoms (except H30A, H30B), and disordered methyl groups on C12, and C26 removed for clarity. Selected bond distances (Å): W1–C30 – 2.172(3), C30–C31 1.530(4), W1–O1 1.8403(19), W1–O2 1.9095(19), W1–O3 1.8345(19), W1–N1 2.015(2), N1–C7 1.474(4), N1–C21 1.404(4), W1–Cl1 2.5221(7). Selected bond angles (deg): ∠W1–C30–C31 126.3(2), ∠W1–O3–C35 161.5(2), ∠N1–W1–O3 168.75(9), ∠O1–W1–O2 160.71(9), ∠C21–N1–C7 112.6(2), ∠C21–N1–W1 116.92(19), ∠C7–N1–W1 130.12(19), ∠C30–W1–Cl1 169.74(9).

Addition of Me$^+$. Unlike complexes $\{\text{CH}_3\text{PPh}_3\}\{[\text{CF}_3\text{-ONO}]\text{W}{\equiv}\text{C}^t\text{Bu(O}^t\text{Bu)}\}$[8] and $\{\text{CH}_3\text{PPh}_3\}\{[\text{OCO}]\text{W}{\equiv}\text{C}^t\text{Bu(O}^t\text{Bu)}\}$,[30] that react with MeOTf to afford the corresponding neutral versions $[\text{CF}_3\text{-ONO}]\text{W}{\equiv}\text{C}^t\text{Bu(OEt}_2)$ and $[\text{OCO}]\text{W}{\equiv}\text{C}^t\text{Bu(OEt}_2)$ respectively, complex **4** reacts with MeOTf to form the N-methylated product, **6-Me** (**Scheme 5**). Unhindered access to the nucleophilic N atom over the $-\text{O}^t\text{Bu}$ was also observed for the flexible ONO ligand in $\{[\text{O}^{\text{CH2}}\text{N}^{\text{CH2}}\text{O}]\text{W}{\equiv}\text{C}^t\text{Bu(O}^t\text{Bu)}\}^-$. Though the inorganic enamine bonding combination in complex **4** places significant electron density at the α-carbon of the alkylidyne, significant electron density in the HOMO orbital resides on the N atom (refer to the HOMO in **Figure 5**). The imido-alkylidyne anion $\{(\text{NAr})\text{Mo}{\equiv}\text{C}^t\text{Bu[OCMe(CF}_3)_2]_2\}^-$ exhibits similar nitrogen-centered reactivity.[60]

Scheme 5. Addition of MeOTf to **4**: Synthesis of **6-Me**

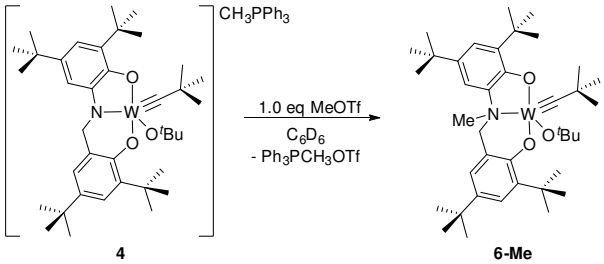

^{1}H NMR spectroscopy establishes the identity of **6-Me**. The methylene protons of the pincer, the W≡C^{t}Bu, and the N-methyl groups serve as important spectroscopic markers. The W≡C^{t}Bu protons in **6-Me** resonate at 0.80 ppm, the methylene protons resonate at 4.78 and 5.49 ppm, and the methyl group

bound to the N atom resonates as a singlet integrating to three protons at 2.05 ppm. Consistent with N-methylation to give an L-type donor,[35] the N atom (observed through ^{1}H-^{15}N *g*HMBC NMR spectroscopy) resonates at 48.9 ppm in **6-Me** as compared to 129.8 ppm for **4**, where the N atom is anionic and an X-type donor.[35] NOESY-1D ^{1}H NMR spectroscopy with selective excitation at 0.80 ppm (W≡C^{t}Bu) shows NOE to one of the methylene protons at 5.49 ppm, thus demonstrating a *syn* orientation, and consequently demonstrates that the N–Me group is *anti* to the alkylidyne ^{t}Bu group.

Addition of TMS+. A useful strategy to displace alkoxide ligands involves stoichiometric addition of a reactive electrophile such as H^{+}.[58] In a unique example, Schrock et al. employed TMSOTf to convert (^{t}BuO)$_3$W≡CAd (where Ad = adamantyl) to (^{t}BuO)$_2$W≡CAd(OTf)(DME).[41] Within our group, MeOTf finds great utility in –O^{t}Bu displacements, such as observed in the syntheses of the complexes [CF$_3$-ONO]W≡C^{t}Bu(OEt$_2$)[8] and [OCO]W≡C^{t}Bu(THF)$_2$.[30] As described above, MeOTf addition to **4** results in N-methylation to generate **6-Me**. To test if a larger electrophile such as TMS^{+} would preferentially silylate the –O^{t}Bu ligand over the pincer N atom, complex **4** was treated with one equivalent of TMSOTf in C_6D_6. Surprisingly, the TMS^{+} also adds to the N atom to generate **6-TMS** (**Scheme 6**), which is somewhat less stable in solution compared to **6-Me**. ^{1}H NMR spectroscopy offers a tool to monitor the reaction progress. The W≡C^{t}Bu resonance shifts upfield from 1.15 ppm for **4** to 0.81 ppm in **6-TMS**, consistent with N-silylation. The TMS group bound to the pincer N atom resonates at 0.01 ppm integrating to nine protons. The methylene protons also deviate from **4**, resonating as doublets centered at 5.29 and 5.53 ppm. The retention of the W≡C^{t}Bu unit is confirmed through a $^{13}C\{^{1}H\}$ resonance at 289.0 ppm.

Scheme 6. Addition of TMSOTf to **4**: synthesis of **6-TMS**

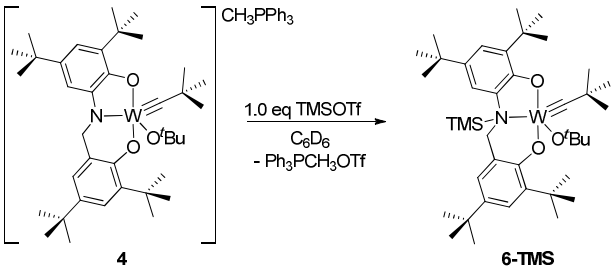

Discussion

DFT computations provide a more comprehensive view of the inorganic enamine bonding interaction within the anionic alkylidynes (**Figure 7**). The extent of separation of the bonding and anti-bonding orbitals for the inorganic enamine interaction in the three alkylidynes essentially follows the order anticipated considering the orientation of the N atom lone pair that was described in **Figure 1** above. The angle between the lone pair of electrons on the N atom and the M-C π-bonds was calculated for {CF$_3$-ONO]WC≡Et(O^{t}Bu)}$^{-}$, {[ON^{CH2}O]W≡C^{t}Bu(O^{t}Bu)}$^{-}$ (**4a**), and {[O^{CH2}N^{CH2}O]W≡C^{t}Bu(O^{t}Bu)}$^{-}$ to be 43°, 14°, and 44°, respectively. Therefore, complex **4a** is expected to have the strongest overlap, and it does with a separation between the HOMO and HOMO(-3) equal to 1.45608 eV. In comparison the rigid ligand in {CF$_3$-ONO]WC≡Et(O^{t}Bu)}$^{-}$, creates the weakest overlap with a separation of only 0.92573 eV. Interestingly, the angle of the N atom lone pair orientation is not the only factor because the flexible ligand has an angle of 44° but creates a strong interaction with a separation between the HOMO and HOMO(-3) of 1.32166 eV. Being flexible the lone pair is still able to orient in space to achieve good overlap.

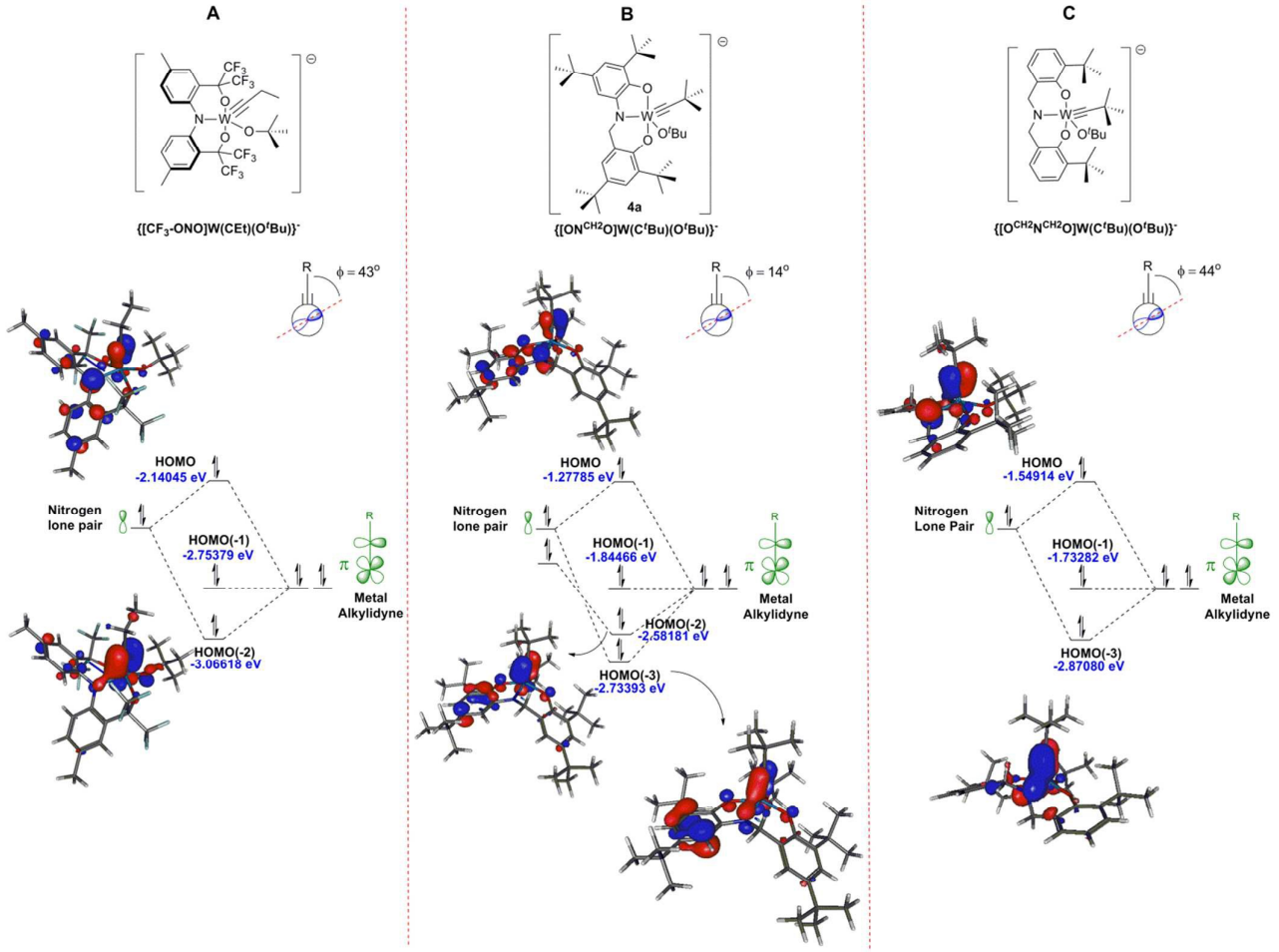

Figure 7. Comparison of the inorganic enamine bonding interaction within W(VI)-alkylidynes ligated to a) $[CF_3\text{-}ONO]^{3-}$ ligand (no spacer), b) $[ON^{CH2}O]^{3-}$ ligand (one spacer flanking the N_{pincer}), and c) $[O^{CH2}N^{CH2}O]^{3-}$ ligand (two spacers flanking the N_{pincer}). All orbital images were generated at isovalue = 0.051687. (B3LYP / LANL2DZ level of theory)

Conclusions

The $[ON^{CH2}O]H_3$ proligand is readily synthesized in gram quantities from a straightforward condensation reaction followed by reduction. Metalation with $(^tBuO)_3W{\equiv}C^tBu$ generates $[ONH^{CH2}O]W{\equiv}C^tBu(O^tBu)$ (**2**) initially, then converts to the neopentylidene $[ON^{CH2}O]W{=}CH^tBu(O^tBu)$ (**3**). Deprotonation of either complex **2** or **3** provides the anionic alkylidyne, $\{CH_3PPh_3\}\{[ON^{CH2}O]W{\equiv}C^tBu(O^tBu)\}$ (**4**). DFT calculations employing the crystallographic coordinates of **4** show strong overlap between the pincer amido lone pair with the alkylidyne π-orbitals in an inorganic enamine bonding combination. Addition of MeOTf to $\{[CF_3\text{-}ONO]W{\equiv}CEt(O^tBu)\}^-$ generates the C_α-alkylated product $[CF_3\text{-}ONO]W{=}C(Me)Et(O^tBu)$; however, for both $\{[O^{CH2}N^{CH2}O]W{\equiv}C^tBu(O^tBu)\}^-$ and **4**, the exposed pincer N atom reacts in preference yielding the N-methylated products (**Scheme 5**). Even a larger electrophile such as the TMS^+ adds to the N atom in **4** (**Scheme 6**). Only the much smaller electrophile H^+ adds to the $W{\equiv}C_\alpha$ bond of **4**; sequentially generating the W(VI)-neopentylidene **3**, and the W(VI)-neopentyl complex, **5** (**Scheme 4**). Even heating **6-Me** and **6-TMS** does not result in migration of the N-substituent to the alkylidyne α-carbon.

Clearly, from an overlap perspective, the inorganic enamine bonding is maximized within $\{[ON^{CH2}O]W{\equiv}C^tBu(O^tBu)\}^-$ (**4a**), and $\{[O^{CH2}N^{CH2}O]W{\equiv}C^tBu(O^tBu)\}^-$ suggesting the methylene spacer is important in aligning the N atom lone pair to be collinear with the alkylidyne π-bonds. In spite of this feature, the anionic alkylidynes supported by the semi-flexible and the flexible ligands suffer from pincer N atom-centered reactivity. This reactivity-pattern is undesirable since access to the neutral alkylidyne is precluded. $\{[CF_3\text{-}ONO]W{\equiv}C^tBu(O^tBu)\}^-$, supported by the rigid ligand exhibits inorganic enamine bonding; yet it cleanly converts to the neutral $[CF_3\text{-}ONO]W{\equiv}C^tBu(OEt_2)$ through MeOTf displacement of the $-O^tBu$ ligand.[7] Within the flexible ligands $[ON^{CH2}O]^{3-}$ and $[O^{CH2}N^{CH2}O]^{3-}$, the exposed N atom reacts in preference to the $M{\equiv}C_\alpha$ bond. Not being able to access the neutral alkylidynes with all three ligands unfortunately does not permit a comprehensive structure/activity relationship. However, the

three ligands, including the newly synthesized semi-flexible version completes the series, and provide for a good spread of ligand architectures that can be exploited in future catalyst designs.

Experimental

General Considerations

Unless specified otherwise, all manipulations were performed under an inert atmosphere using standard Schlenk or glove-box techniques. Glassware was oven dried before use. Pentane, hexane, toluene, diethyl ether (Et_2O), tetrahydrofuran (THF), benzene (C_6H_6) were dried using a GlassContours drying column and stored over 4 Å molecular sieves. Benzene-d_6 (Cambridge Isotopes) was dried over sodium-benzophenone ketyl, distilled and stored over 4 Å molecular sieves. Toluene-d_8 (Cambridge Isotopes) was dried over CaH_2; vacuum transferred and stored over 4 Å molecular sieves. THF-d_8 (Cambridge Isotopes) was used as received. (^{t}BuO)$_3$W≡C^{t}Bu,[2, 61] 2-amino-4,6-di-tert-butylphenol,[12-15] 3,5-di-tert-butyl-2-hydroxybenzaldehyde,[16-18] 2,4-di-tert-butyl-6-((3,5-di-tert-butyl-2-hydroxybenzylidene)amino)phenol,[19-23] and $Ph_3P{=}CH_2$[36] were prepared according to published procedures. All other reagents were purchased from commercial vendors and used without further purification. ^{1}H, ^{13}C{^{1}H}, and 2D NMR spectra were obtained on an Inova 500 MHz spectrometer, and ^{31}P{^{1}H} NMR spectra was acquired on a Varian Mercury Broad Band 300 MHz, or Varian Mercury 300 MHz spectrometers. The chemical shifts are reported in δ (ppm) and were referenced to the lock signal on the TMS scale for ^{1}H and ^{13}C NMR spectra, and neat NH_3 scale for ^{15}N NMR spectra. For ^{1}H and ^{13}C{^{1}H} NMR spectra, the residual solvent peak was used as an internal reference. Elemental analyses were performed at Complete Analysis Laboratory Inc., Parsippany, New Jersey.

DFT Calculations

Geometry optimization and single point analysis of **4a** were performed using spin-restricted density functional theory calculations, using a hybrid functional B3LYP[53-54] and LANL2DZ[55] basis as implemented in the Gaussian 09[56] program suite. The atomic coordinates from the crystal structure of **4** were used as an initial input for the geometry optimized structure **4a**. Molecular orbital pictures of **4a** were generated from Gabedit[57] at the reported isovalue.

Synthesis of [ON^{CH2}O]H$_3$ (1)

In a well-ventilated fume hood, under ambient conditions, 2,4-di-tert-butyl-6-((3,5-di-tert-butyl-2-hydroxybenzylidene)amino)phenol (6.57 g, 15.0 mmol) was suspended in 100 mL of ethanol (200 proof) and chilled using an ice-water bath. To this cold, rapidly stirring suspension, 2.27 g of $NaBH_4$ (60.0 mmol, 4 equiv) was added using a spatula in portions (time interval of 10 - 15 seconds between the additions). By the end of the addition, the reaction mixture color turned from yellow to deep red-orange. After 10 min of stirring at this temperature, the reaction mixture was refluxed under argon for 2 h. During the reflux the solution color changed to deep purple. The reflux was stopped, the reaction mixture was allowed to reach ambient temperature, and then quenched by addition of an excess of 1N HCl until fuming ceased. The reaction mixture changed from purple to off-white. Water was added to dilute the reaction mixture and then the organic phase was extracted three times with dichloromethane. The golden colored organic phase was dried using $MgSO_4$, filtered, and the solvent was removed in vacuo. A single pentane trituration gave a cream colored solid (Yield = 4.99 g, 69.7%), identified as the hydrochloride salt, **1·HCl**. The hydrochloride salt **1·HCl** (3.03 g, 6.36 mmol) was dissolved in 75 mL of methanol, and a methanolic solution of NaOMe (0.351 g of NaOMe$_{(s)}$, 6.36 mmol) was added in drops using a pipette. The color changed from hazy yellow to a homogeneous yellow solution. After 45 min of stirring, the solvent was removed in vacuo, and extracted with acetonitrile. Filtration, in vacuo removal of solvent, and pentane trituration afforded **1** as a pale-yellow solid which was further purified by recrystallization from pentane. (Yield = 1.45 g, 51.8%) ^{1}H NMR (C_6D_6, 500 MHz): δ = 7.51 (d, 1H, $^4J_{HH}$ = 1.9 Hz, Ar-*H*), 7.10 (d, 1H, $^4J_{HH}$ = 1.9 Hz, Ar-*H*), 6.94 (d, 1H, $^4J_{HH}$ = 1.9 Hz, Ar-*H*), 6.83 (d, 1H, $^4J_{HH}$ = 1.9 Hz, Ar-*H*), 3.89 (s, 2H, C*H*$_2$), 1.65 (s, 9H, Ar-C(C*H*$_3$)$_3$), 1.40 (s, 9H, Ar-C(C*H*$_3$)$_3$), 1.39 (s, 9H, Ar-C(C*H*$_3$)$_3$), 1.29 (s, 9H, Ar-C(C*H*$_3$)$_3$) ppm. ^{13}C{^{1}H} (75 MHz, C_6D_6): δ = 154.2 (s, Ar), 143.5 (s, Ar), 143.3 (s, Ar), 141. 7 (s, Ar), 136.6 (s, Ar), 136.3 (s, Ar), 136.0 (s, Ar), 124.2 (s, Ar), 123.5 (s, Ar), 123.3 (s, Ar), 116.9 (s, Ar), 113.2 (s, Ar), 50.8 (s, -*C*H$_2$-), 35.4 (s, Ar-*C*(CH$_3$)$_3$), 34.8 (s, Ar-*C*(CH$_3$)$_3$), 34.7 (s, Ar-*C*(CH$_3$)$_3$), 34.5 (s, Ar-*C*(CH$_3$)$_3$), 32.0 (s, Ar-C(*C*H$_3$)$_3$), 31.9 (s, Ar-C(*C*H$_3$)$_3$), 30.2 (s, Ar-C(*C*H$_3$)$_3$), 30.1 (s, Ar-C(*C*H$_3$)$_3$) ppm. ^{15}N NMR (From ^{1}H-^{15}N *g*HMBC, 500 MHz, C_6D_6): δ = 50.0 ppm. HRMS (ESI-TOF) m/z: [M+H]$^+$ Calcd for $C_{29}H_{46}NO_2$ 440.3523; Found 440.3532

Synthesis of [ONH^{CH2}O]W≡C^{t}Bu(O^{t}Bu) (2) and [ON^{CH2}O]W=CH^{t}Bu(O^{t}Bu) (3)

In a glove box, a scintillation vial with **1** (100 mg, 0.227 mmol) in 2 mL of benzene was added to a benzene solution of (^{t}BuO)$_3$W≡C^{t}Bu (111 mg, 0.235 mmol, 1.03 equiv) at ambient temperature and allowed to stir. After 30 min, all volatiles were evaporated under vacuum for 1 h. The resulting red-brown powder was dissolved in pentane and filtered through a Celite® plug. The red-brown powder was identified as [ON***H***^{CH2}O]W≡C^{t}Bu(O^{t}Bu) (**2**) using ^{13}C{^{1}H}NMR spectroscopy. Warming a C_6D_6 solution of complex **2** to 70 °C facilitated proton migration from the amino backbone to the alkylidyne fragment affording [ON^{CH2}O]W=C***H***^{t}Bu(O^{t}Bu) (**3**). (Total Yield = 119 mg, 68.6%)

[ON***H***^{CH2}O]W≡C^{t}Bu(O^{t}Bu) (2)

^{1}H NMR (C_7D_8, 500 MHz, – 30 °C): δ = 7.54 (d, 1H, $^4J_{HH}$ = 1.9 Hz, Ar-*H*), 7.40 (d, 1H, $^4J_{HH}$ = 1.9 Hz, Ar-*H*), 7.09 (d, 1H, $^4J_{HH}$ = 1.9 Hz, Ar-*H*), 7.04 (d, 1H, $^4J_{HH}$ = 1.9 Hz, Ar-*H*), 4.97 (dd, 1H, $^2J_{HH}$ = 14.0 Hz, $^3J_{HH}$ = 12.9 Hz, C*H*$_2$), 4.78 (dd, 1H, $^2J_{HH}$ = 14.0 Hz, $^3J_{HH}$ = 1.8 Hz, C*H*$_2$), 2.79 (br, 1H, N*H*), 1.78 (s, 9H, Ar-C(C*H*$_3$)$_3$), 1.77 (s,

9H, Ar-C(CH_3)$_3$), 1.76 (s, 9H, Ar-C(CH_3)$_3$), 1.37 (s, 9H, Ar-C(CH_3)$_3$), 1.36 (s, 9H, Ar-C(CH_3)$_3$), 0.82 (s, 9H, W≡C(CH_3)$_3$) ppm. ^{13}C NMR (indirect detection from ^{1}H-^{13}C *g*HMBC) (C_7D_8, 500 MHz, − 30 °C): δ = 288.5 (W≡*C*C(CH$_3$)$_3$), 160.3 (Ar-*C*), 159.2 (Ar-*C*), 140.5 (Ar-*C*), 138.9 (Ar-*C*), 137.4 (Ar-*C*), 136.4 (Ar-*C*), 135.8 (s, Ar-*C*), 122.5 (Ar-*C*), 122.0 (Ar-*C*), 121.7 (Ar-*C*), 121.0 (Ar-*C*), 113.8 (Ar-*C*), 79.4 (O*C*(CH$_3$)$_3$), 55.6 (*C*H$_2$), 50.0 (W≡C*C*(CH$_3$)$_3$), 35.2 (Ar-*C*(CH$_3$)$_3$), 34.9 (Ar-*C*(CH$_3$)$_3$), 34.3 (Ar-*C*(CH$_3$)$_3$), 34.1 (Ar-*C*(CH$_3$)$_3$), 33.2 (OC(*C*H$_3$)$_3$), 33.1 (W≡CC(*C*H$_3$)$_3$), 31.6 (Ar-C(*C*H$_3$)$_3$), 30.0 (Ar-C(*C*H$_3$)$_3$), 29.3 (s, Ar-C(*C*H$_3$)$_3$) ppm.^{15}N NMR (From ^{1}H-^{15}N *g*HMBC, 500 MHz, C_7D_8, − 30 °C): δ = 48.1 ppm. Anal. Calcd. for $C_{38}H_{61}NO_3W$: C, 59.76%; H, 8.05%; N, 1.83%. Found: C, 59.70%; H, 7.92%; N, 2.04%

[ON^{CH2}O]W=C*H*^{t}Bu(O^{t}Bu) (3)

^{1}H NMR (C_6D_6, 500 MHz): δ = 8.90 (s, 1H, $^2J_{WH}$ = 15 Hz, W=C*H*(C(CH$_3$)$_3$)), 7.50 (d, 1H, $^4J_{HH}$ = 2.4 Hz, Ar-*H*), 7.30 (d, 1H, $^4J_{HH}$ = 2.4 Hz, Ar-*H*), 7.20 (d, 1H, $^4J_{HH}$ = 2.4 Hz, Ar-*H*), 7.07 (d, 1H, $^4J_{HH}$= 2.4 Hz, Ar-*H*), 5.46 (d, 1H, $^2J_{HH}$ = 16.7 Hz, C*H*$_2$), 5.08 (d, 1H, $^2J_{HH}$ = 16.7 Hz, CH$_2$), 1.75 (s, 9H, Ar-C(C*H*$_3$)$_3$), 1.74 (s, 9H, Ar-C(C*H*$_3$)$_3$), 1.45 (s, 9H, Ar-C(C*H*$_3$)$_3$)), 1.43 (s, 9H, -OC(C*H*$_3$)$_3$)), 1.34 (s, 9H, Ar-C(C*H*$_3$)$_3$)), 0.68 (s, 9H, W=CH(C(C*H*$_3$)$_3$)) ppm. ^{13}C{^{1}H} NMR (C_6D_6, 125 MHz): δ = 255.6 (s, W=*C*HC(CH$_3$)$_3$)), 160.7 (s, Ar-*C*), 155.0 (s, Ar-*C*), 146.0 (s, Ar-*C*), 142.1 (s, Ar-*C*), 141.8 (s, Ar-*C*), 135.0 (s, Ar-*C*), 134.9 (s, Ar-*C*), 128.4 (s, Ar-*C*), 122.2 (s, Ar-*C*), 116.3 (s, Ar-*C*), 107.1 (s, Ar-*C*), 84.5 (s, -O*C*(CH$_3$)$_3$), 53.8 (s, *C*H$_2$), 44.6 (s, W=CH*C*(CH$_3$)$_3$), 35.1 (s, Ar-*C*(CH$_3$)$_3$), 34.6 (s, Ar-*C*(CH$_3$)$_3$), 34.2 (s, Ar-*C*(CH$_3$)$_3$), 33.7 (s, W=CHC(*C*H$_3$)$_3$), 32.1 (s, Ar-C(*C*H$_3$)$_3$), 31.6 (s, Ar-C(*C*H$_3$)$_3$), 30.8 (s, OC(*C*H$_3$)$_3$), 30.2 (s, Ar-C(*C*H$_3$)$_3$), 30.0 (s, Ar-C(*C*H$_3$)$_3$) ppm. ^{15}N NMR (From ^{1}H-^{15}N *g*HMBC, 500 MHz, C_6D_6): δ = 260.6 ppm. Anal. Calcd. for $C_{38}H_{61}NO_3W$: C, 59.76%; H, 8.05%; N, 1.83%. Found: C, 59.70%; H, 7.92%; N, 2.04%

Synthesis of {MePPh$_3$}{[ON^{CH2}O]W≡C^{t}Bu(O^{t}Bu)} (4)

A pentane solution (5 mL) of **3** (173 mg, 0.227 mmol, 1.0 equiv) was added in drops to the rapidly stirring pentane solution of $Ph_3P{=}CH_2$ (75 mg, 0.27 mmol, 1.2 equiv); an immediate color change from yellow to orange was observed with the formation of a precipitate. The reaction mixture was stirred for 4 hours before being filtered through a medium porosity frit. The orange residue was washed with pentane thrice and dried in vacuo to remove volatiles. (Yield = 0.23 g, 96%) Crystals suitable for X-ray crystallography were grown from pentane diffusion into a concentrated THF solution of **4**.

^{1}H NMR (C_6D_6, 500 MHz, 25 °C): δ = 7.45 (d, 1H, $^3J_{HH}$ = 2.2 Hz, Ar-*H*), 7.27 (d, 1H, $^3J_{HH}$ = 2.2 Hz, Ar-*H*), 7.10 (br, 3H, Ar-*H*), 7.00 (br, 7H, Ar-*H*), 6.83 (d, 1H, $^3J_{HH}$ = 1.8 Hz), 6.68 (d, 1H, $^3J_{HH}$ = 1.8 Hz), 5.37 (d, 1H, $^2J_{HH}$ = 15.7 Hz), 5.05 (d, 1H, $^2J_{HH}$ = 15.7 Hz), 2.01 (s, 9H, OC(C*H*$_3$)$_3$), 1.84 (s, 9H, Ar-C(C*H*$_3$)$_3$), 1.80 (s, 9H, Ar-C(C*H*$_3$)$_3$), 1.46 (s, 9H, Ar-C(C*H*$_3$)$_3$), 1.39 (s, 9H, Ar-C(C*H*$_3$)$_3$), 1.15 (s, 9H, W≡C(C*H*$_3$)$_3$) ppm. ^{13}C{^{1}H} NMR (C_6D_6, 125 MHz, 25 °C): δ = 290.6 (s, W≡*C*(C(CH$_3$)$_3$)), 161.5 (s, Ar-*C*), 156.0 (s, Ar-*C*), 153.1 (s, Ar-*C*), 138.4 (s, Ar-*C*), 137.3 (s, Ar-*C*), 136.6 (s, Ar-*C*), 134.3 (s, Ar-*C*), 132.4 (d, $^3J_{CP}$ = 10.9 Hz), 131.2 (s, Ar-*C*), 130.0 (d, $^3J_{CP}$ = 10.9 Hz), 129.4 (s, Ar-*C*), 122.4 (s, Ar-*C*), 120.1 (s, Ar-*C*), 118.7 (d, J_{CP} = 82.1 Hz), 107.0 (s, Ar-*C*), 102.6 (s, Ar-*C*), 76.5 (s, O*C*(CH$_3$)$_3$), 54.1 (s, *C*H$_2$), 49.1 (s, W≡C(*C*(CH$_3$)$_3$)), 35.7 (s, Ar-*C*(CH$_3$)$_3$), 35.2 (s, W≡C(C(CH$_3$)$_3$)), 34.8 (s, Ar-*C*(CH$_3$)$_3$), 34.6 (s, Ar-*C*(CH$_3$)$_3$), 34.1 (s, Ar-*C*(CH$_3$)$_3$), 34.1 (s, OC(*C*H$_3$)$_3$), 32.6 (s, Ar-C(*C*H$_3$)$_3$), 32.1 (s, Ar-C(*C*H$_3$)$_3$), 30.7 (s, Ar-C(*C*H$_3$)$_3$), 30.2 (s, Ar-C(*C*H$_3$)$_3$) ppm. ^{15}N NMR (From ^{1}H-^{15}N *g*HMBC, 500 MHz, C_6D_6): δ = 130.0 ppm. ^{31}P{^{1}H} NMR (121 MHz, C_6D_6): δ = 21.3 ppm (bs). Anal. Calcd. for $C_{57}H_{78}NO_3PW$: C, 65.82%; H, 7.56%; N, 1.35%. Found: C, 65.69%; H, 7.34%; N, 1.57%.

Synthesis of [ON^{CH2}O]W(CH$_2$C(CH$_3$)$_3$)(O^{t}Bu)Cl (5)

In the glove-box, (^{t}BuO)$_3$W≡C^{t}Bu (163 mg, 0.345 mmol) in 2 mL C_6H_6 was added in drops to a C_6H_6 suspension of **1·HCl** (161 mg, 0.338 mmol) and mixed well with a pipette. The deep brown-red suspension became homogeneous within fifteen minutes of stirring at ambient temperature. After the reaction mixture was stirred for 15 h, all volatiles were removed in vacuo, leaving behind a deep brown residue. Pentane trituration, performed three times, and extensive drying yields **5**. (Yield = 220 mg, 80.9%). Crystals suitable for X-ray interrogation can be grown by the slow evaporation of a concentrated diethyl ether solution of **5** at ambient temperature. Complex **5** can also be accessed through addition of 2 equiv of HCl in Et_2O to **4**.

^{1}H NMR (300 MHz, C_6D_6, 25 °C): δ = 7.49 (d, 1H, $^4J_{HH}$ = 2.3 Hz, Ar-*H*), 7.22 (d, 1H, $^4J_{HH}$ = 2.3 Hz, Ar-*H*), 6.75 (d, 1H, $^4J_{HH}$ = 1.8 Hz, Ar-*H*), 6.65 (d, 1H, $^4J_{HH}$ = 1.8 Hz, Ar-*H*), 6.64 (d, 1H, $^2J_{HH}$ = 20.4 Hz, NC*H*$_2$), 6.29 (d, 1H, $^2J_{HH}$ = 20.4 Hz, NC*H*$_2$), 2.41 (d, 1H, $^2J_{HH}$ = 14.1 Hz, WC*H*$_2$^{t}Bu), 2.20 (d, 1H, $^2J_{HH}$ = 14.1 Hz, WC*H*$_2$^{t}Bu), 1.75 (s, 9H, OC(C*H*$_3$)$_3$), 1.62 (s, 9H, Ar-C(C*H*$_3$)$_3$), 1.56 (s, 9H, Ar-C(C*H*$_3$)$_3$), 1.26 (s, 9H, Ar-C(C*H*$_3$)$_3$), 1.24 (s, 9H, Ar-C(C*H*$_3$)$_3$), 0.96 (s, 9H, WCH$_2$(C(C*H*$_3$)$_3$)) ppm. ^{13}C{^{1}H} NMR (125 MHz, C_6D_6, 25 °C): δ = 155.5 (s, Ar-*C*), 150.9 (s, Ar-*C*), 149.8 (s, Ar-*C*), 147.1 (s, Ar-*C*), 146.2 (s, Ar-*C*), 137.4 (s, Ar-*C*), 135.2 (s, Ar-*C*), 128.3 (s, Ar-*C*), 123.2 (s, Ar-*C*), 123.2 (s, Ar-*C*), 123.0 (s, Ar-*C*), 109.4 (s, Ar-*C*), 93.5 (s, WC*H*$_2$^{t}Bu), 90.1 (s, O*C*(CH$_3$)$_3$), 52.7 (s, N*C*H$_2$), 37.4 (s, WCH$_2$(*C*(CH$_3$)$_3$)), 35.5 (s, Ar(*C*(CH$_3$)$_3$)), 34.9 (s, Ar(*C*(CH$_3$)$_3$)), 34.8 (s, Ar(*C*(CH$_3$)$_3$)), 34.7 (s, WCH$_2$(C(*C*H$_3$)$_3$)), 32.0 (s, Ar(C(*C*H$_3$)$_3$)), 31.6 (s, Ar(C(*C*H$_3$)$_3$)), 30.8 (s, Ar(C(*C*H$_3$)$_3$)), 30.2 (s, OC(*C*H$_3$)$_3$), 30.0 ppm (s, Ar(C(*C*H$_3$)$_3$)) ppm. ^{15}N NMR (From ^{1}H-^{15}N *g*HMBC, 500 MHz, C_6D_6, 25 °C): δ = 299.8 ppm. Anal. Calcd. for $C_{38}H_{62}ClNO_3W$: C, 57.04%; H, 7.81%; N, 1.75%. Found: C, 56.99%; H, 7.94%; N, 2.01%.

In situ solution-phase experiments:

6-Me

To a C_6D_6 solution (0.8 mL) of **4** (120 mg, 0.115 mmol) in a vial, cold MeOTf (12.7 µL, 0.115 mmol) was added in two portions (2 x 6.3 µL). The reaction mixture showed no appreciable color change. The reaction mixture was stirred for 4 h and then filtered into a J-Young NMR tube for 2D-NMR interrogation.

The same reaction can be performed in pentane. In pentane, an immediate color change from orange to brown was observed upon addition of MeOTf with the formation of a precipitate. After 2 h of stirring, the reaction mixture was filtered, and the volatiles were removed in vacuo to afford a brown residue identified as **6-Me**. ^{1}H NMR (C_6D_6, 500 MHz): δ

= 7.58 (d, 1H, $^4J_{HH}$ =3.0 Hz, Ar-*H*), 7.40 (d, 1H, $^4J_{HH}$ = 3.0 Hz, Ar-*H*), 7.20 (d, 1H, $^4J_{HH}$ = 3.0 Hz, Ar-*H*), 7.14 (d, 1H, $^4J_{HH}$ = 3.0 Hz, Ar-*H*), 5.49 (d, 1H, $^2J_{HH}$ = 14.0 Hz, CH_2), 4.78 (d, 1H, $^2J_{HH}$ = 14.0 Hz, CH_2), 2.05 (s, 3H, NCH_3), 1.75 (s, 9H, Ar-C(CH_3)$_3$), 1.75 (s, 9H, OC(CH_3)$_3$), 1.73 (s, 9H, Ar-C(CH_3)$_3$), 1.36 (s, 9H, Ar-C(CH_3)$_3$), 1.33 (s, 9H, Ar-C(CH_3)$_3$), 0.80 (s, 9H, W≡C(CH_3)$_3$) ppm. ^{13}C NMR (From ^{1}H-^{13}C *g*HMBC NMR spectrum, C_6D_6, 500 MHz): δ = 288.7 (W≡*C*C(CH$_3$)$_3$), 159.1 (Ar-*C*), 158.3 (Ar-*C*), 144.6 (Ar-*C*), 141.7 (Ar-*C*), 140.5 (Ar-*C*), 138.3 (Ar-*C*), 136.8 (Ar-*C*), 123.0 (Ar-*C*), 122.7 (Ar-*C*), 121.6 (Ar-*C*), 121.2 (Ar-*C*), 111.1 (Ar-*C*), 80.0 (-O*C*(CH$_3$)$_3$), 64.1 (*C*H$_2$), 50.3 (W≡C*C*(CH$_3$)$_3$), 47.1 (NCH$_3$). 35.4 (Ar-*C*(CH$_3$)$_3$), 35.2 (Ar-*C*(CH$_3$)$_3$), 34.4 (Ar-*C*(CH$_3$)$_3$), 34.1 (Ar-*C*(CH$_3$)$_3$), 33.0 (OC(*C*H$_3$)$_3$), 32.9 (W≡CC(*C*H$_3$)$_3$), 31.7 (Ar-C(*C*H$_3$)$_3$), 31.6 (Ar-C(*C*H$_3$)$_3$), 30.1 (Ar-C(*C*H$_3$)$_3$), 29.5 (Ar-C(*C*H$_3$)$_3$) ppm.^{15}N NMR: (From ^{1}H-^{15}N *g*HMBC, 500 MHz, C_6D_6): δ = 48.9 ppm

6-TMS

To a pentane suspension (2.0 mL) of **4** (52 mg, 0.055 mmol), TMSOTf (10 µL, 0.055 mmol) was added in drops. The orange suspension turned brown upon addition of TMSOTf with copious precipitation. The reaction mixture was stirred for an hour, filtered, and the volatiles were removed in vacuo to yield **6-TMS** as a brown powder. ^{1}H NMR (C_6D_6, 500 MHz): δ = 7.53 (d, 1H, $^4J_{HH}$ =2.2 Hz, Ar-*H*), 7.33 (d, 1H, $^4J_{HH}$ = 2.2 Hz, Ar-*H*), 7.18 (d, 1H, $^4J_{HH}$ = 2.2 Hz, Ar-*H*), 7.14 (d, 1H, $^4J_{HH}$ = 2.2 Hz, Ar-*H*), 5.53 (d, 1H, $^2J_{HH}$ = 14.4 Hz, CH_2), 5.29 (d, 1H, $^2J_{HH}$ = 14.4 Hz, CH_2), 1.73 (s, 9H, OC(CH_3)$_3$), 1.72 (s, 18H, Ar-C(CH_3)$_3$), 1.36 (s, 9H, Ar-C(CH_3)$_3$), 1.35 (s, 9H, Ar-C(CH_3)$_3$), 0.81 (s, 9H, W≡C(CH_3)$_3$), 0.01 (s, 9H, NSi(CH_3)$_3$) ppm. ^{13}C{^{1}H} NMR (C_6D_6, 125 MHz): δ = 289.0 (s, W≡*C*C(CH$_3$)$_3$), 161.6 (s, Ar-*C*), 159.2 (s, Ar-*C*), 141.5 (s, Ar-*C*), 141.4 (s, Ar-*C*), 139.5 (s, Ar-*C*), 137.5 (s, Ar-*C*), 135.9 (s, Ar-*C*), 124.5 (s, Ar-*C*), 122.0 (s, Ar-*C*), 121.9 (s, Ar-*C*), 119.7 (s, Ar-*C*), 114.9 (s, Ar-*C*), 79.9 (s, -O*C*(CH$_3$)$_3$), 60.8 (s, *C*H$_2$), 50.1 (s, W≡C*C*(CH$_3$)$_3$), 35.3 (s, Ar-*C*(CH$_3$)$_3$), 34.9 (s, Ar-*C*(CH$_3$)$_3$), 34.2 (s, Ar-*C*(CH$_3$)$_3$), 34.1 (s, Ar-*C*(CH$_3$)$_3$), 33.1 (s, W≡CC(*C*H$_3$)$_3$), 32.9 (s, OC(*C*H$_3$)$_3$), 31.6 (s, Ar-C(*C*H$_3$)$_3$), 31.6 (s, Ar-C(*C*H$_3$)$_3$), 30.1 (s, Ar-C(*C*H$_3$)$_3$), 29.4 (s, Ar-C(*C*H$_3$)$_3$), -0.6 (s, NSi(*C*H$_3$)$_3$) ppm. ^{15}N NMR: δ = not measured

Acknowledgements

A.S.V. thanks the University of Florida for financial support of this project. This material is based upon work supported by the National Science Foundation CHE-1265993. K.A.A. thanks the University of Florida and the National Science Foundation (CHE-0821346) for funding the purchase of X-ray equipment. Computational resources and support were provided by the University of Florida High-Performance Computing Center.

Notes and references

The [ON^{CH2}O]H$_3$ ligand, based on the similarity of its design to other redox active ligands, can potentially be non-innocent. The complexes prepared in this report do not exploit this possibility, but it is an active area of investigation.

1 S. Beer, C. G. Hrib, P. G. Jones, K. Brandhorst, J. Grunenberg and M. Tamm, *Angew. Chem. Int. Ed.*, 2007, **46**, 8890-8894.
2 S. Beer, K. Brandhorst, C. G. Hrib, X. Wu, B. Haberlag, J. Grunenberg, P. G. Jones and M. Tamm, *Organometallics*, 2009, **28**, 1534-1545.
3 X. Wu, C. G. Daniliuc, C. G. Hrib and M. Tamm, *J. Organomet. Chem.*, 2011, **696**, 4147-4151.
4 K. Y. Shih, K. Totland, S. W. Seidel and R. R. Schrock, *J. Am. Chem. Soc.*, 1994, **116**, 12103-12104.
5 F. V. Cochran and R. R. Schrock, *Organometallics*, 2001, **20**, 2127-2129.
6 R. R. Schrock, J. Y. Jamieson, J. P. Araujo, P. J. Bonitatebus, A. Sinha, L. Pia and H. Lopez, *J. Organomet. Chem.*, 2003, **684**, 56-67.
7 M. E. O'Reilly, I. Ghiviriga, K. A. Abboud and A. S. Veige, *J. Am. Chem. Soc.*, 2012, **134**, 11185-11195.
8 M. E. O'Reilly, I. Ghiviriga, K. A. Abboud and A. S. Veige, *Dalton Trans.*, 2013, **42**, 3326-3336.
9 S. VenkatRamani, N. B. Huff, M. T. Jan, I. Ghiviriga, K. A. Abboud and A. S. Veige, *Organometallics*, 2015, **34**, 2841-2848.
10 (Ed.) G. A. Cook, *Enamines: Synthesis, Structure, And Reactivity*, Macel Dekker, Inc, 1988.
11 S. A. Gonsales, M. E. Pascualini, I. Ghiviriga, K. A. Abboud and A. S. Veige, *J. Am. Chem. Soc.*, 2015, **137**, 4840-4845.
12 F. Dulong, O. Bathily, P. Thuery, M. Ephritikhine and T. Cantat, *Dalton Trans.*, 2012, **41**, 11980-11983.
13 T. M. Khomenko, O. V. Salomatina, S. Y. Kurbakova, I. V. Il'ina, K. P. Volcho, N. I. Komarova, D. V. Korchagina, N. F. Salakhutdinov and A. G. Tolstikov, *Russ. J. Org. Chem.*, 2006, **42**, 1653-1661.
14 V. I. Lodyato, I. L. Yurkova, V. L. Sorokina, O. I. Shadyro, V. I. Dolgopalets and M. A. Kisel, *Bioorg. Med. Chem. Lett.*, 2003, **13**, 1179-1182.
15 J. Vinsova, K. Cermakova, A. Tomeckova, M. Ceckova, J. Jampilek, P. Cermak, J. Kunes, M. Dolezal and F. Staud, *Biorg. Med. Chem.*, 2006, **14**, 5850-5865.
16 N. U. Hofslokken and L. Skattebol, *Acta. Chem. Scand.*, 1999, **53**, 258-262.
17 J. F. Larrow and E. N. Jacobsen, *Organic Syntheses, Vol 75*, 1998, **75**, 1-11.
18 G. F. Moore, J. D. Megiatto, Jr., M. Hambourger, M. Gervaldo, G. Kodis, T. A. Moore, D. Gust and A. L. Moore, *Photoch. Photobio. Sci.*, 2012, **11**, 1018-1025.
19 A. Abreu, S. J. Alas, H. I. Beltran, R. Santillan and N. Farfan, *J. Organomet. Chem.*, 2006, **691**, 337-348.
20 V. V. Lukov, A. A. Knysh, S. N. Lyubchenko, Y. P. Tupolova and V. A. Kogan, *Russ. J. Coord. Chem.*, 2002, **28**, 874-876.
21 T. Tanaka, M. Koyama, S. Ikegami and M. Koga, *Bull. Chem. Soc. Jpn.*, 1972, **45**, 630-632.
22 S. Y. S. Wang, J. M. Boncella and K. A. Abboud, *Acta Crystallogr., Sect. C: Cryst. Struct. Commun.*, 1997, **53**, 436-438.
23 T. Xu, J. Liu, G.-P. Wu and X.-B. Lu, *Inorg. Chem.*, 2011, **50**, 10884-10892.
24 N. Zhao, L. Chen, W. S. Ren, H. B. Song and G. F. Zi, *J. Organomet. Chem.*, 2012, **712**, 29-36.
25 M. L. Listemann and R. R. Schrock, *Organometallics*, 1985, **4**, 74-83.
26 M. Karplus, *J. Chem. Phys.*, 1959, **30**, 11-15.
27 M. Karplus, *J. Am. Chem. Soc.*, 1963, **85**, 2870-2871.
28 B. Haberlag, X. Wu, K. Brandhorst, J. Grunenberg, C. G. Daniliuc, P. G. Jones and M. Tamm, *Chem. Eur. J.*, 2010, **16**, 8868-8877.
29 S. Lysenko, C. G. Daniliuc, P. G. Jones and M. Tamm, *J. Organomet. Chem.*, 2013, **744**, 7-14.

30 S. Sarkar, K. P. McGowan, S. Kuppuswamy, I. Ghiviriga, K. A. Abboud and A. S. Veige, *J. Am. Chem. Soc.*, 2012, **134**, 4509-4512.
31 K. P. McGowan, M. E. O'Reilly, I. Ghiviriga, K. A. Abboud and A. S. Veige, *Chem. Sci.*, 2013, **4**, 1145-1155.
32 M. E. O'Reilly, S. S. Nadif, I. Ghiviriga, K. A. Abboud and A. S. Veige, *Organometallics*, 2014, **33**, 836-839.
33 M. E. O'Reilly and A. S. Veige, *Chem. Soc. Rev.*, 2014, **43**, 6325-6369.
34 S. A. Gonsales, M. E. Pascualini, I. Ghiviriga, K. A. Abboud and A. S. Veige, *J. Am. Chem. Soc.*, 2015, **137**, 4840-4845.
35 M. L. H. Green and G. Parkin, *J. Chem. Educ.*, 2014, **91**, 807-816.
36 H. J. Bestmann, W. Stransky and O. Vostrowsky, *Chem. Ber. Recl.*, 1976, **109**, 1694-1700.
37 A. W. Addison, T. N. Rao, J. Reedijk, J. Vanrijn and G. C. Verschoor, *J. Chem. Soc., Dalton Trans.*, 1984, 1349-1356.
38 Z. J. Tonzetich, Y. C. Lam, P. Müller and R. R. Schrock, *Organometallics*, 2007, **26**, 475-477.
39 M. R. Churchill and W. J. Youngs, *Inorg. Chem.*, 1979, **18**, 2454-2458.
40 M. R. Churchill, Y. J. Li, L. Blum and R. R. Schrock, *Organometallics*, 1984, **3**, 109-113.
41 T. H. Warren, R. R. Schrock and W. M. Davis, *J. Organomet. Chem.*, 1998, **569**, 125-137.
42 P. Doufou, K. A. Abboud and J. M. Boncella, *Inorg. Chim. Acta*, 2003, **345**, 103-112.
43 J. C. Jeffery, J. A. McCleverty, M. D. Mortimer and M. D. Ward, *Polyhedron*, 1994, **13**, 353-356.
44 M. H. Chisholm, D. M. Hoffman and J. C. Huffman, *Inorg. Chem.*, 1983, **22**, 2903-2906.
45 M. H. Chisholm, B. K. Conroy and J. C. Huffman, *Organometallics*, 1986, **5**, 2384-2386.
46 M. H. Chisholm, B. W. Eichhorn, K. Folting and J. C. Huffman, *Organometallics*, 1989, **8**, 49-66.
47 M. H. Chisholm, J. C. Huffman and J. A. Klang, *Polyhedron*, 1990, **9**, 1271-1276.
48 F. A. Cotton and W. Schwotzer, *Inorg. Chem.*, 1983, **22**, 387-390.
49 F. A. Cotton, W. Schwotzer and E. S. Shamshoum, *Organometallics*, 1984, **3**, 1770-1771.
50 H. A. Brison, T. P. Pollagi, T. C. Stoner, S. J. Geib and M. D. Hopkins, *Chem. Commun.*, 1997, 1263-1264.
51 T. P. Pollagi, S. J. Geib and M. D. Hopkins, *J. Am. Chem. Soc.*, 1994, **116**, 6051-6052.
52 S. M. Rocklage, R. R. Schrock, M. R. Churchill and H. J. Wasserman, *Organometallics*, 1982, **1**, 1332-1338.
53 A. D. Becke, *J. Chem. Phys.*, 1993, **98**, 5648-5652.
54 C. T. Lee, W. T. Yang and R. G. Parr, *Phys. Rev. B*, 1988, **37**, 785-789.
55 P. J. Hay and W. R. Wadt, *J. Chem. Phys.*, 1985, **82**, 270-283.
56 M. J. Frisch, G. W. Trucks, H. B. Schlegel, G. E. Scuseria, M. A. Robb, J. R. Cheeseman, G. Scalmani, V. Barone, B. Mennucci, G. A. Petersson, H. Nakatsuji, M. Caricato, X. Li, H. P. Hratchian, A. F. Izmaylov, J. Bloino, G. Zheng, J. L. Sonnenberg, M. Hada, M. Ehara, K. Toyota, R. Fukuda, J. Hasegawa, M. Ishida, T. Nakajima, Y. Honda, O. Kitao, H. Nakai, T. Vreven, J. A. Montgomery Jr., J. E. Peralta, F. Ogliaro, M. J. Bearpark, J. Heyd, E. N. Brothers, K. N. Kudin, V. N. Staroverov, R. Kobayashi, J. Normand, K. Raghavachari, A. P. Rendell, J. C. Burant, S. S. Iyengar, J. Tomasi, M. Cossi, N. Rega, N. J. Millam, M. Klene, J. E. Knox, J. B. Cross, V. Bakken, C. Adamo, J. Jaramillo, R. Gomperts, R. E. Stratmann, O. Yazyev, A. J. Austin, R. Cammi, C. Pomelli, J. W. Ochterski, R. L. Martin, K. Morokuma, V. G. Zakrzewski, G. A. Voth, P. Salvador, J. J. Dannenberg, S. Dapprich, A. D. Daniels, Ö. Farkas, J. B. Foresman, J. V. Ortiz, J. Cioslowski and D. J. Fox, Gaussian, Inc., Wallingford, CT, USA, 2009.
57 A.-R. Allouche, *J. Comput. Chem.*, 2011, **32**, 174-182.
58 J. H. Freudenberger and R. R. Schrock, *Organometallics*, 1985, **4**, 1937-1944.
59 D. N. Clark and R. R. Schrock, *J. Am. Chem. Soc.*, 1978, **100**, 6774-6776.
60 Z. J. Tonzetich, R. R. Schrock and P. Muller, *Organometallics*, 2006, **25**, 4301-4306.
61 M. L. Listemann and R. R. Schrock, *Organometallics*, 1985, **4**, 74-83.